Mechanical Design Optimization of a Pneumatically Actuated Parallel Kinematic Machine

Klemens Springer[1], Hubert Gattringer[2] and Andreas Müller[2]

***Abstract*— The application field of motion simulation needs robotic platforms with a high level of dexterity payload. Therefore increasingly parallel manipulators/platforms are used as 3 to 6 degree-of-freedom constructions. The contradictory aim for high applicable forces and large workspace volumes necessitates an optimization of the mechanical construction. In contrast to common configurations the robot utilized here is a hexapod equipped with antagonistic type of pneumatic actuation, imitating the flexor-extensor principle of human muscles. A counter force is applied passively through a spring in the center point of the hexapod. This structure offers advantages for application as motion simulator such as little maintenance requirements and low cost assembly. Due to the direct correlation between actuator length and dynamics, the use of classical techniques for workspace evaluation in the area of design optimization is not applicable. The paper illustrates the optimal design of this parallel kinematic machine concerning maximum workspace taking into account the dynamical system. The presented method ensures stability in the upper maximum possible position through an additional optimization of the maximum disturbance force. The resulting multi-objective optimization problem is solved by using an evolutionary algorithm with a Pareto approach. The introduced method for evaluating an adequate measure of the maximum workspace volume for parallel platforms is well suited in the application field of motion simulators. The optimal solutions of the Pareto front are evaluated and compared to the parameters used in the existing configuration of the platform at the Institute of Robotics.**

Keywords: multi-objective optimization, parallel robots, design optimization, motion simulator, pneumatic actuation

I. INTRODUCTION

Parallel kinematic machines have received growing attention in the fields of vibration damping, medical surgery and industrial applications like toolheads in the last few years, see [1], [2]. Originally invented for motion simulation (see [3], [4]), which is the purpose here as well (Fig. 1), hexapods have successfully asserted themselves in this area. Following the most accurate definition *Gough platform* is used for the parallel platform. The main advantages, good accuracy and dexterity, of a Gough platform accompany the disadvantage of small workspace, which is most important for the given application. Thus a main aim within the mechanical design of these platforms is the maximization of the workspace volume without loosing the advantageous properties, see [5], [6], [7]. In the last years a lot of research has been done in the optimization of the dynamic behavior and compliance by Zhang in [8], stiffness by Krefft in [9], manipulability by Wen in [10] and general workspace maximization with respect to constructive constraints by Masory in [11]. Hardly any attention has been paid to mechanical design optimization concerning antagonistic actuation systems with a passive component. This article introduces new techniques for the workspace optimization of a pneumatically actuated 6-degree of freedom Gough platform including dynamical considerations. That necessity results from the direct correlation between the kinematics (contraction) and dynamics (pressure) of the actuator. Due to the lack of the possibility to impress forces of arbitrary directions by the pneumatic actuators, see Fig. 2, a spring is mounted in the center of the construction to passively apply opposite forces and torques. In order to maximize the possible disturbance force at the topmost pose, an additional objective criteria is introduced for avoiding the loss of manipulability. Countless authors addressed single-objective optimizations of parallel mechanisms. This approach leads to a dominant problem for the present contradictory formulation. To find an appropriate solution, it is formulated as a multi-objective optimization problem. Genetic algorithms, that are predestined for non-convex and non-smooth optimization formulations, use evolutionary strategies from genetic programming to cope these types of problems, see [12], [13]. In contrast to standard gradient-based solvers, they have no need for gradient information, are nearly independent of discontinuities and are more efficient in performing a global search. To allow for multi-objective considerations, a Pareto approach in combination with genetic algorithms is used.

In accordance with the contents presented above, this paper

Fig. 1: Motion simulator mounted on the parallel platform

[1]Klemens Springer, Engel Austria GmbH, 4311 Schwertberg, Austria
[2] Hubert Gattringer, Andreas Müller are with Institute of Robotics, Johannes Kepler University Linz, 4040 Linz, Austria {hubert.gattringer,a.mueller} @jku.at

https://doi.org/10.34749/3061-0710.2025.2

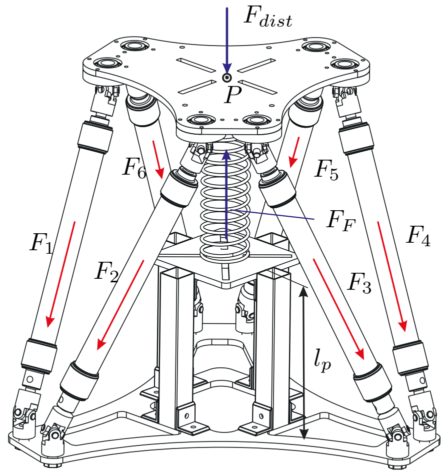

Fig. 2: Possible directions of actuator and spring forces

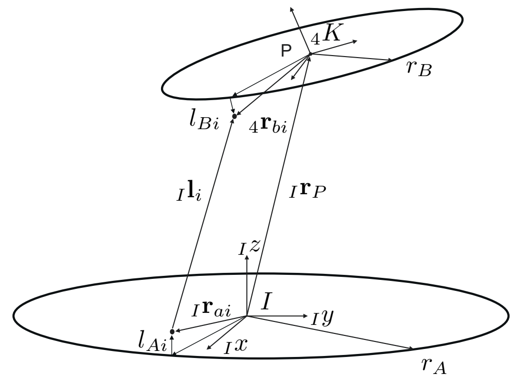

Fig. 3: Coordinate systems and kinematics for one arm

is arranged as follows. After a description of the modeling of the mechatronic system including kinematical and dynamical considerations (section 2), the formulation of the optimization problem is shown in section 3. Introducing new techniques, the calculation of the workspace and maximum disturbance force is illustrated. Section 4 focuses on the explanation and implementation of the problem formulation through a genetic programming based solver with a Pareto approach for multi-objective considerations. Furthermore the results of the optimization are presented. At the end of the paper in section 5 a conclusion for the used technique is drawn.

II. Modeling of the mechatronic system

The considered mechatronic system is split into a kinematical and a dynamical section, containing the pneumatic subsystem as well.

A. Kinematic description

The considered robot consists of two rigid platforms - the fixed base and the movable, coaxially arranged, upper one. They are connected by six flexible pneumatically driven fluidic actuators and a spring in the center of the robot, see again Fig. 2 . This concept is based on the principle of the human muscle system, whereby here the opponent to the muscles is a passive one. The inertial coordinate system is chosen in the center of the base platform. In order to calculate the maximum workspace, the inverse kinematics, that describes the actuator lengths in dependence of the Cartesian coordinates of the tool center point P, is needed. For this, the solution of ${}_I\mathbf{l}_i = {}_I\mathbf{r}_P + \mathbf{R}_{I4}\ {}_4\mathbf{r}_{bi} - {}_I\mathbf{r}_{ai}$ has to be found (see Fig. 3), where the endpoint vector ${}_I\mathbf{r}_P$ is equivalent to the first three entries of the minimal coordinates $\mathbf{q} = \begin{bmatrix} x & y & z & \alpha & \beta & \gamma \end{bmatrix}^T$.

There, the angles α, β, and γ represent the rotation of the upper platform in Cardan description and x, y, z the position relative to the inertial coordinate system. The rotation matrix $\mathbf{R}_{I4}$ relates the body-fixed coordinate system ${}_4K$ in the center of the upper platform to the inertial frame. The vectors ${}_I\mathbf{r}_{ai}$ and ${}_4\mathbf{r}_{bi}$ to the actuator contact points are calculated as functions of the optimization variables r_A, r_B (radii of the mounting mounts of the actuators), α_{off} and β_{off} (offset angles), shown in Fig. 4 and Fig. 3.

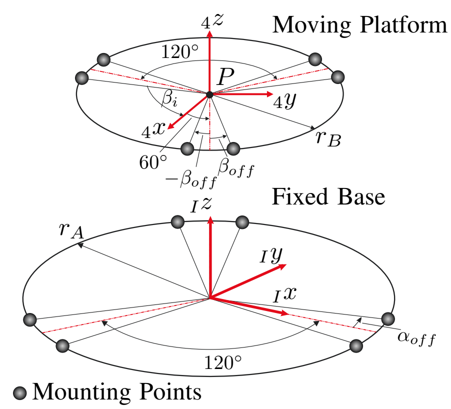

Fig. 4: Angular offsets

Constraints: For respecting constructive constraints, the maximum actuator lengths $l_{max} = l_0\,(1+0.05)$, $l_{min} = l_0\,(1-0.25)$, given by the manufacturer's specifications, and passive joint angles

$$\begin{aligned} \theta_{A,i_{Min}} \leq \theta_{A,i} = \cos^{-1}\left({}_I\mathbf{e}_3^T\,{}_I\mathbf{u}_i\right) \leq \theta_{A,i_{Max}} \quad , \quad i = 1\cdots 6 \\ \theta_{B,i_{Min}} \leq \theta_{B,i} = \cos^{-1}\left({}_4\mathbf{e}_3^T\,{}_I\mathbf{u}_i\right) \leq \theta_{B,i_{Max}} \quad , \quad i = 1\cdots 6 \end{aligned} \tag{1}$$

with the actuator direction vectors and the unit vectors in the respective coordinate systems

$$\begin{aligned} {}_I\mathbf{u}_i &= \frac{{}_I\mathbf{l}_i}{\|{}_I\mathbf{l}_i\|} = \frac{{}_I\mathbf{r}_P + \mathbf{R}_{I4}\ {}_4\mathbf{r}_{bi} - {}_I\mathbf{r}_{ai}}{\|{}_I\mathbf{r}_P + \mathbf{R}_{I4}\ {}_4\mathbf{r}_{bi} - {}_I\mathbf{r}_{ai}\|} \quad , \quad i = 1\cdots 6 \\ {}_I\mathbf{e}_3^T &= [0,0,1] \quad , \quad {}_4\mathbf{e}_3^T = [0,0,1] \end{aligned} \tag{2}$$

have to be formulated (Fig. 5). The pneumatic actuators have a nominal length of l_0 and are fixed with universal joints, mounted in axial bearings, in the upper platform. As a consequence of this additional degree of freedom, the upper universal joints do not constrain the maximum angles

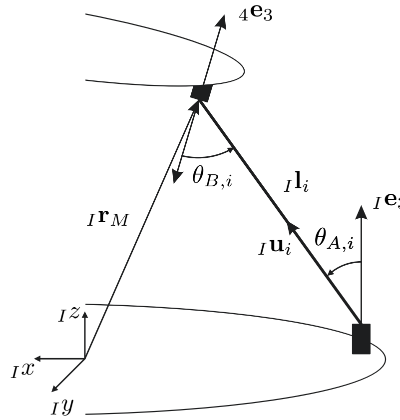

Fig. 5: Kinematic constraints for joint angles

of inclination $\theta_{B,i} = 90°$. In contrast to this, only $60°$ are allowed for the universal joints' inclination angles $\theta_{A,i}$ at the base platform. Actuator collisions can be neglected because other constraints become active before they would occur.

B. Dynamical description

The equations of motion in minimal description are calculated with the projection equation, see [14] and results in

$$\begin{aligned}\mathbf{M}(\mathbf{q})\ddot{\mathbf{q}} + \mathbf{g}(\mathbf{q},\dot{\mathbf{q}}) + \mathbf{K}\mathbf{q} &= \mathbf{Q}_m = \mathbf{B}(\mathbf{q})\mathbf{F}_m \\ \mathbf{F}_m &= [F_1, F_2, .., F_6]^T\end{aligned} \tag{3}$$

see [15] for details. $\mathbf{M}(\mathbf{q})$ is the mass matrix, and $\mathbf{g}(\mathbf{q},\dot{\mathbf{q}})$ contains the remaining nonlinear terms (gravity, centrifugal, Coriolis). $\mathbf{K}$ represents the stiffness matrix due to the spring forces. The generalized driving forces $\mathbf{Q}_m$ can be separated into the input matrix $\mathbf{B}(\mathbf{q})$ and the actuator forces $\mathbf{F}_m$. These actuator forces are projected into the minimal space by

$$\mathbf{Q}_m = \sum_{i=1}^{6} \mathbf{J}_{m,i}^T \; {}_I\mathbf{u}_i \; F_i. \tag{4}$$

The partial derivatives of the vectors to the actuator mount base ${}_I\mathbf{r}_{Mi}$, see Fig. 5, yield the Jacobian

$$\mathbf{J}_{m,i} = \frac{\partial_I \mathbf{r}_{Mi}}{\partial \mathbf{q}} = \frac{\partial \left({}_I\mathbf{r}_P + \mathbf{R}_{I4} \; {}_4\mathbf{r}_{bi}\right)}{\partial \mathbf{q}}, \quad i = 1 \dots 6. \tag{5}$$

Eq. (4) can be combined to

$$\mathbf{Q}_m = \mathbf{B}(\mathbf{q})\mathbf{F}_m. \tag{6}$$

1) Pneumatic subsystem: The 6 pneumatic subsystems consist of a fluidic actuator by FESTO, called fluidic muscle, an analog proportional valve, a pressure sensor and a linear potentiometer to measure the actuator lengths $\|{}_I\mathbf{l}_i\|_2$. The muscles are made of a fiber-reinforced rubber tube with mounting flanges at the ends. The actuator operates as follows: Air flows into the tube and leads to increasing pressure $p_i, \; i = 1 \dots 6$ and thus to a broadening of the muscle. Because of specially arranged fibers this results in a contraction h of the muscle

$$h_i = \frac{l_{0,i} - \|{}_I\mathbf{l}_i\|_2}{l_{0,i}} 100\%, \quad i = 1 \dots 6 \tag{7}$$

in percent in longitudinal direction with the relaxed link length $l_{0,i}$ of muscle i. This fact is used to generate pulling forces

$$F_i = \left(p_i \sum_{k=1}^{n_a} a_k h_i^k + \sum_{k=1}^{n_b} b_k h_i^k \right), \quad i = 1 \dots 6 \tag{8}$$

that have nonlinear characteristics and depend on the pressures p_i and the contractions h_i. The polynomial coefficients $a_k, \; b_k$ are derived from a mathematical approximation of the actuator's characteristics given by the manufacturer, see Fig. 6.

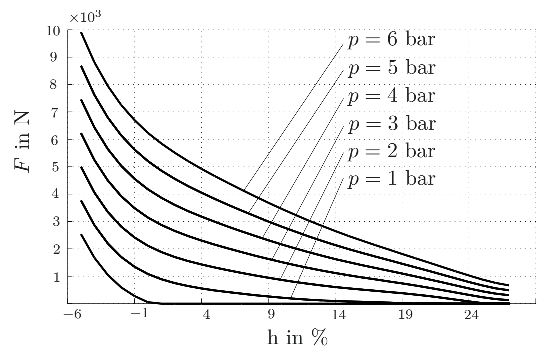

Fig. 6: Characteristics of the fluidic muscle DMSP40 by FESTO

2) Identification of the spring parameters: In order to describe the dynamical model from section II-B as exact as possible, which is needed for the optimization formulation, the spring parameters have to be known. Therefore an identification of the stiffness matrix $\mathbf{K}$ is done based one the Least Squares method, see [16] for details. This identification was verified through calculating a feedforward control based on the identified spring stiffness matrix and evaluating the position error. The error is around $0.5mm$ in the middle of the workspace and not much higher in the topmost and the lowest pose.
Since the identification is only done relative to the one set of muscles used for the measurement and the specified repeatability is $\leq 1\%$, the inaccuracy of the actuators does not influence the spring identification. More sophisticated models of the spring using neuronal networks can be found in [17].

III. Optimization Problem

As discussed extensively in numerous publications, the most important optimization criterion in the process of mechanical design of parallel kinematic machines is the maximization of the workspace. Commonly the workspace is iteratively evaluated with a method, based on the inverse kinematic of the Gough platform, see e.g. [11]. Different from this approach an application adequate measure is used here as a substitution for the workspace volume. This simplification balances out the increased calculation effort caused by the necessary consideration of the actuator dynamics while resulting in a quality of the solution that is sufficient for motion

https://doi.org/10.34749/3061-0710.2025.2

simulation. Furthermore the orientation is included in the used application adequate measure.

A. Workspace

Due to the high complexity of the analytical calculation of the workspace, a numerical approach similar to that in [11], has been chosen. Based on the assumption, that the volume of the cubage can be approached with $V_{AR} = \frac{1}{3}(x_{max} - x_{min})\big|_{z=z_{mid}} (y_{max} - y_{min})\big|_{z=z_{mid}} (z_{max} - z_{min})$ with the workspace center $z_{mid} = (z_{min} + z_{max})/2$, the maximum translational displacements x_{min}, x_{max}, y_{min}, y_{max}, z_{min} and z_{max} have to be calculated. Therefore the actuator lengths of 6 reference poses

$$
\begin{aligned}
\mathbf{q}_{P_1} &= [0, 0, z_{min}, 0, 0, 0] \\
\mathbf{q}_{P_2} &= [0, 0, z_{max}, 0, 0, 0] \\
\mathbf{q}_{P_3} &= [x_{min}, 0, z_{mid}, 0, 0, 0] \\
\mathbf{q}_{P_4} &= [x_{max}, 0, z_{mid}, 0, 0, 0] \\
\mathbf{q}_{P_5} &= [0, y_{min}, z_{mid}, 0, 0, 0] \\
\mathbf{q}_{P_6} &= [0, y_{max}, z_{mid}, 0, 0, 0]
\end{aligned}
\tag{9}
$$

are evaluated with respect to the length and joint angle constraints. Only constraints concerning the lower joint angles have to be considered. The procedure is introduced briefly:

1) Starting at an infeasible point, e.g. $\mathbf{q}_P = [\mathbf{0}]$, the actuator lengths and joint angles for an increasing z coordinate are iteratively calculated. The first point that does not violate the constraints represents the minimum displacement z_{min}.
2) Starting at $\mathbf{q}_{P_1}$ the z coordinate is increased again and the actuator lengths and joint angles are iteratively calculated. If the constraints are violated, the last feasible position reveals the maximum displacement z_{max}. Hence the relative displacement $\Delta z = (z_{max} - z_{min})$ is calculated.
3) Next the actuator lengths and joint angles are calculated for positions with increasing displacements in the x and y coordinates one axis after the other, starting at the workspace center $(\mathbf{q}_{P_1} + \mathbf{q}_{P_2})/2$. If the constraints are violated, the last feasible position reveals the maximum displacement x_{max} or y_{max}.
4) The same way x_{min} and y_{min} are computed with decreasing displacements starting at the workspace center, which from $\Delta x = (x_{max} - x_{min})$ and $\Delta y = (y_{max} - y_{min})$ ensues.

On the basis of this algorithm, an objective function for evaluating an application adequate measure as approximation for the workspace volume of this hexapod, treated as a rigid mechanism, can be suggested. The calculation of the maximum positions starting at $(\mathbf{q}_{P_1} + \mathbf{q}_{P_2})/2$ is completely admissible in the specific application field of a motion simulator, whose default position is at $\mathbf{q}_0 = (\mathbf{q}_{P_1} + \mathbf{q}_{P_2})/2$. The optimization variables to manipulate this measure are the platform radii r_A, r_B and the offset angles α_{off}, β_{off}, see Fig. 4. Reconsidering the direct correlation between impressed force and contraction of the pneumatic actuators, it comes clear that not only kinematics have to be kept in mind, but also the dynamic modeling and a dynamic mass calculation due to variable platform radius r_B. Consequently, the workspace calculation has to be extended and the maximum positions are calculated with respect to dynamics. Regarding this problem statically with $\dot{\mathbf{q}}$, $\ddot{\mathbf{q}} = \mathbf{0}$, the actuator forces

$$
\begin{aligned}
&\mathbf{F}_m(\mathbf{q}, \dot{\mathbf{q}} = \mathbf{0}, \ddot{\mathbf{q}} = \mathbf{0}) = \\
&\quad \mathbf{B}(\mathbf{q})^{-1}\Big(\underbrace{\mathbf{M}(\mathbf{q})\,\ddot{\mathbf{q}}}_{\mathbf{0}} + \mathbf{g}(\mathbf{q}, \mathbf{0}) + \mathbf{K}\mathbf{q}\Big) \\
&\mathbf{F}_m(\mathbf{q}) = \mathbf{B}(\mathbf{q})^{-1}\Big(\mathbf{K}\mathbf{q} + \mathbf{g}(\mathbf{q}, \mathbf{0})\Big)
\end{aligned}
\tag{10}
$$

are calculated via the inverse dynamics. Hence and in combination with the muscle contractions at the current position gained via inverse kinematics and Eqn. (7), the required muscle pressures

$$
p_i = \frac{F_i - \sum_{k=1}^{n_b} b_k h_i^k}{\sum_{k=1}^{n_a} a_k h_i^k}, \quad i = 1 \dots 6 \tag{11}
$$

are determined. If the pressure constraints $0 \leq p_i \leq p_{max} = 6bar$, given by manufacturer specifications, are violated, then the displacement $z_{min,act} = z_{min,act} + \Delta z_{red}$, exemplary shown for the minimum displacement in z-direction, is reduced consecutively by a minimal value Δz_{red} till a feasible position is found.

In order to include the orientation in this measure, the maximum rotatory displacements $\boldsymbol{\phi}$, analogously to the workspace volume evaluation, are calculated in 6 reference poses

$$
\begin{aligned}
\mathbf{q}_{P_7} &= [0, 0, z_{mid}, \alpha_{min}, 0, 0] \\
\mathbf{q}_{P_8} &= [0, 0, z_{mid}, \alpha_{max}, 0, 0] \\
\mathbf{q}_{P_9} &= [0, 0, z_{mid}, 0, \beta_{min}, 0] \\
\mathbf{q}_{P_{10}} &= [0, 0, z_{mid}, 0, \beta_{max}, 0] \\
\mathbf{q}_{P_{11}} &= [0, 0, z_{mid}, 0, 0, \gamma_{min}] \\
\mathbf{q}_{P_{12}} &= [0, 0, z_{mid}, 0, 0, \gamma_{max}] .
\end{aligned}
\tag{12}
$$

Hence $\Delta\alpha = (\alpha_{max} - \alpha_{min})$, $\Delta\beta = (\beta_{max} - \beta_{min})$ and $\Delta\gamma = (\gamma_{max} - \gamma_{min})$ result. Now the workspace evaluation function can be stated as

$$
\begin{aligned}
\Psi_{AR} &= \frac{1}{2}W_{11}\Delta x^2 + \frac{1}{2}W_{22}\Delta y^2 + \frac{1}{2}W_{33}\Delta z^2 + \\
&\quad \frac{1}{2}W_{44}\Delta\alpha^2 + \frac{1}{2}W_{55}\Delta\beta^2 + \frac{1}{2}W_{66}\Delta\gamma^2 \\
&= \frac{1}{2}\begin{bmatrix}\Delta\mathbf{r}^T & \Delta\boldsymbol{\phi}^T\end{bmatrix}\mathbf{W}\begin{bmatrix}\Delta\mathbf{r} \\ \Delta\boldsymbol{\phi}\end{bmatrix} = \frac{1}{2}\Delta\mathbf{q}^T\mathbf{W}\Delta\mathbf{q} \\
\mathbf{W} &\geq 0
\end{aligned}
\tag{13}
$$

with the positive definite diagonal weighting matrix $\mathbf{W} = diag(0.5, 0.5, 5, 0.5, 0.5, 0.05)$ and the diagonal entries W_{ii}. The maximum displacements are represented with $\Delta\mathbf{r}^T = [x_{max} - x_{min},\ y_{max} - y_{min},\ z_{max} - z_{min}]$ and $\Delta\boldsymbol{\phi}^T = [\alpha_{max} - \alpha_{min},\ \beta_{max} - \beta_{min},\ \gamma_{max} - \gamma_{min}]$.

In the application of a motion simulator, gravity is used for simulating sustaining accelerations through tilting the pilot's seat. Therefore defined minimum required rotations $[\alpha_{lb}, \alpha_{ub}] = [-10°, 10°]$ and $[\beta_{lb}, \beta_{ub}] = [-10°, 10°]$ are postulated for the roll angle α and the pitch angle β, that are considered through an unequality constraint

$$\Psi_{AR,c} = \begin{cases} \Psi_{AR} & \alpha_{max} > \alpha_{ub} \ \wedge \ \alpha_{min} < \alpha_{lb} \ \wedge \\ & \beta_{max} > \beta_{ub} \ \wedge \ \beta_{min} < \beta_{lb} \\ 0 & \text{else} \end{cases} \tag{14}$$

implemented in a constrained workspace evaluation function.

B. Disturbance force

Numerous publications concerning research in stiffness, compliance and dynamical optimization can be found, see [8], [9], [10], as mentioned in the introductory section. These considerations are featuring minor optimization potential for the used Gough platform, because of only one variable dynamic parameter (upper platform mass) and the predominant structural compliance due to the fluidic muscles and the spring. Another challenging peculiarity of this construction is the one-way force direction of the actuators. As a consequence a force impression in positive z direction in the upper reference pose $\mathbf{q}_{P_2}$ is not possible if an adequate pretension of the spring through the parameter l_p, see Fig. 2, is missing. Therefore the maximum possible disturbance force in negative z direction $F_{dist,max}$ has to be optimized with l_p as optimization variable. The force

$$\begin{aligned} F_{dist,max} &= \mathbf{e}_3^T \sum_{i=1}^{6} \mathbf{J}_{m,i}^T \ {}_I\mathbf{u}_i \Delta F_i \\ \mathbf{e}_3^T &= [0,0,1,0,0,0] \end{aligned} \tag{15}$$

results out of the maximum applicable muscle forces ΔF_i with the Jacobian $\mathbf{J}_{m,i}$ for the transmission of the generalized forces, see Eqn. (5), and the unit vectors ${}_I\mathbf{u}_i$, see Eqn. (2) and Fig. 5. The required actuator forces

$$\Delta F_i = F_i(p_{min,i}) - F_i(p_{0,i}), \quad i = 1 \dots 6 \tag{16}$$

are gained out of the drive forces, see Eqn. (8), in the upper reference pose $\mathbf{q}_{P_2}$ with the unknown pressure

$$p_{min,i} = p\left(F_i\left(\mathbf{q} = \mathbf{q}_{P_2}, F_{dist} = F_{dist,max}\right), h_i(\mathbf{q}_{P_2})\right) \tag{17}$$

occurring at the impression of the unknown maximum disturbance force and the pressure

$$p_{0,i} = p\left(F_i\left(\mathbf{q} = \mathbf{q}_{P_2}, F_{dist} = 0\right), h_i(\mathbf{q}_{P_2}\right) \tag{18}$$

occurring in the absence of the disturbance force, see Eqn. (11). The needed forces in joint space $\mathbf{F}_m \in \mathbb{R}^6$ are a result of an adapted inverse dynamic, formulated out of Eqn. (10) with an additional disturbance term F_{dist}

$$\mathbf{F}_m\left(\mathbf{q}, F_{dist}\right) = \mathbf{B}(\mathbf{q})^{-1}\left(\mathbf{K}\mathbf{q} + \mathbf{g}(\mathbf{q},\mathbf{0}) - F_{dist}\mathbf{e}_3\right). \tag{19}$$

In order to calculate $p_{min,i}$ we need to know that in the topmost position at least one actuator holds a relative pressure of p_{min} = 0 bar when the maximum controllable disturbance is impressed. Hence the maximum pressure reserve

$$\Delta p = \min_i \{0 - p_{0,i}\} \tag{20}$$

due to the muscle pressure constraints, mentioned in section III-A is determined. Furthermore, the muscle forces can be expressed with $p_{min,i} = p_{0,i} + \Delta p$ and the evaluation of Eqn. (16) and Eqn. (8) to

$$\Delta F_i = \Delta p \sum_{k=1}^{n_a} a_k h_d^k, \quad i = 1 \dots 6. \tag{21}$$

If force impressions of arbitrary directions are desired, then the maximum pressure reserve is computed to

$$\Delta p = \min_i \left\{ \frac{(0 - p_{0,i})}{\frac{\partial p_i}{\partial F_{dist}}} \right\} \frac{\partial p_i}{\partial F_{dist}}, \quad i = 1 \dots 6 \tag{22}$$

with the pressure rate gained through a difference approximation

$$\begin{aligned} \frac{\partial p_i}{\partial F_{dist}} &= \frac{p_{\Delta F_{dist},i} - p_{0,i}}{\Delta F_{dist}}, \quad i = 1 \dots 6 \\ p_{\Delta F_{dist},i} &= p\left(F_i\left(\mathbf{q} = \mathbf{q}_{P_2}, F_{dist} = \Delta F_{dist}\right), h_i(\mathbf{q}_{P_2})\right), \end{aligned} \tag{23}$$

and a small disturbance force ΔF_{dist}. With the evaluation of Eqn. (15) the second objective function is defined as well.

C. Optimization Problem

The overall optimization problem can now specified as

$$\begin{aligned} \max_{\mathbf{x}} \ & J_1 = \Psi_{AR,c} \\ \max_{\mathbf{x}} \ & J_2 = F_{dist,max} \\ \text{s.t.} \ & r_B \le r_A \\ & \underline{\mathbf{x}} \le \mathbf{x} \le \overline{\mathbf{x}} \end{aligned} \tag{24}$$

with the optimization variables $\mathbf{x} = [r_A, r_B, \alpha_{off}, \beta_{off}, l_p]$ that are bounded to lower bounds $\underline{\mathbf{x}}$ and upper bounds $\overline{\mathbf{x}}$.

IV. Optimization Procedure

The formulation of Eqn. (24) describes a multi-objective optimization problem. The objectives J_1 and J_2 behave contradictory, whereby a multicriterial approach is needed for finding an appropriate solution. Therefore a Pareto approach is applied, because using one objective function as a result of a *direct weight assignment* method for example does not describe a physical representation. The solver used here is the existent and versatile solver *gamultiobj* in *Matlab*. The resulting Pareto front in Fig. 7, that represents the number of non-dominated solutions, shows the dominance of the maximized disturbance force, evaluated in the objective function J_2. Despite this fact, an applicable set of solutions has been found through the Pareto approach. The Pareto front also reveals solutions that allow very high disturbance forces in the upper maximum pose. Based on a maximum load of 150 kg, the parameters with the biggest workspace volume measure $\Psi_{AR,c}$ and sufficient $F_{dist,max}$ are gained out. Important for the construction in the application field of motion simulation are mainly the parameters $\Delta z, \Delta\alpha$ and $\Delta\beta$, as it emerges from the weighting values in section

https://doi.org/10.34749/3061-0710.2025.2

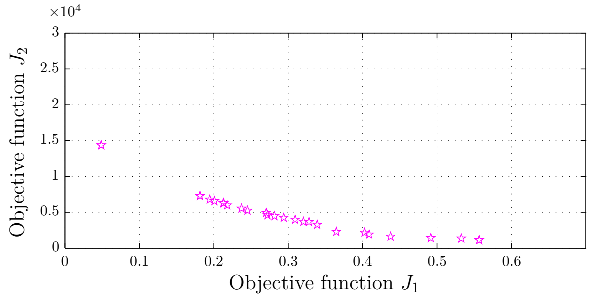

Fig. 7: Pareto front

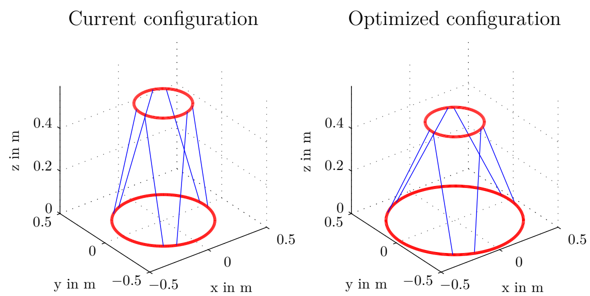

Fig. 8: Comparison between the current and one optimized configuration for the Gough platform

III-A, in order to simulate high-frequency up and down movements and sustaining accelerations through utilizing the gravitational vector. In comparison to the current configuration of the Gough platform at the Institute of Robotics, a huge improvement in the important degrees of freedom is achieved. This comparison of the resulting constructions is illustrated in Fig. 8, that shows the expected behavior. The narrower the construction is, the higher is the maximum applicable disturbance force and the more expanded the platform is, the bigger the workspace measure will get.

V. Conclusion

Optimizing the kinematic design parameters of the construction is a traidoff between maximizing the admissible disturbance forces at the upper extremal position and maximizing the workspace. In the decision making process for the choice of a solution from the Pareto front, a compromise was made. Furthermore the combination of kinematics and actuator dynamics involves challenging difficulties. It was shown that, despite the pneumatic actuator dynamics, a workspace optimization with a maximization of the admissible disturbance force was possible using the methods of genetic algorithms in combination with a Pareto approach concerning multi-objective optimization formulations.

ACKNOWLEDGMENT

This work has been supported by the “LCM – K2 Center for Symbiotic Mechatronics” within the framework of the Austrian COMET-K2 program.

References

[1] J. P. Merlet, *Parallel Robots (Solid Mechanics and Its Applications)*, 2nd ed. Springer, 2001. [Online]. Available: http://www.worldcat.org/isbn/1402003854

[2] A. Müller, “Parallel robots,” in *Robotics Goes MOOC*, B. Siciliano, Ed. Springer, 2025, pp. 89–165.

[3] K. L. Cappel, “Motion simulator,” US Patent RE27 051, 1964.

[4] D. Stewart, “A platform with six degrees of freedom,” in *Proceedings of the Institution of Mechanical Engineers*, vol. 180, 1965, pp. 371–386.

[5] J. P. Merlet, “Determination of 6d workspaces of gough-type parallel manipulator and comparison between different geometries,” *The International Journal of Robotics Research*, vol. 18, no. 9, pp. 902–916, 1999. [Online]. Available: http://ijr.sagepub.com/content/18/9/902.abstract

[6] D. Kim, W. Chung, and Y. Youm, “Geometrical approach for the workspace of 6-dof parallel manipulators,” in *Proceedings of the IEEE International Conference on Robotics and Automation*, vol. 4, 1997, pp. 2986 –2991.

[7] M. Badescu and C. Mavroidis, “Workspace optimization of 3-legged upu and ups parallel platforms with joint constraints,” *ASME Journal of Mechanical Design*, vol. 126, pp. 291–300, 2004.

[8] D. Zhang, Z. Xu, C. M. Mechefske, and F. Xi, “Optimum design of parallel kinematic toolheads with genetic algorithms,” *Robotica*, vol. 22, pp. 77 – 84, 2004. [Online]. Available: http://portal.acm.org/citation.cfm?id=976500.976508

[9] M. Krefft and J. Hesselbach, “Elastodynamic optimization of parallel kinematics,” in *Proceedings of the IEEE International Conference on Automation Science and Engineering*, 2005, pp. 357 – 362.

[10] J. Wen and L. Wilfinger, “Kinematic manipulability of general constrained rigid multibody systems,” *IEEE Transactions on Robotics and Automation*, vol. 15, pp. 1020 –1025, 1999.

[11] O. Masory and J. Wang, “Workspace evaluation of stewart platforms,” *Advanced Robotics*, vol. 9, pp. 443–461, 1995.

[12] M. Gen and R. Cheng, *Genetic Algorithms and Engineering Optimization (Engineering Design and Automation)*. Wiley-Interscience, 1999. [Online]. Available: http://www.worldcat.org/isbn/0471315311

[13] S. Stan, M. Manic, R. Balan, and V. Maties, “Genetic algorithms for workspace optimization of planar medical parallel robot,” in *Proceedings of the IEEE International Conference on Emerging Trends in Computing*, 2009.

[14] H. Bremer, *Elastic Multibody Dynamics: A Direct Ritz Approach*, G. Tzafestas, Ed. Springer-Verlag GmbH, 2008.

[15] H. Gattringer, R. Naderer, and H. Bremer, “Modeling and control of a pneumatically driven stewart platform,” in *Motion and Vibration Control*, 2009, pp. 93 – 102.

[16] H. Trogmann, *Neue Regelverfahren für eine pneumatische Stewart Plattform*. Masterarbeit, Johannes Kepler Universität Linz, 2009.

[17] S. Gadringer, C. Mayr, H. Gattringer, and A. Mueller, “Neural network feedforward control for pneumatic hexapod excavator simulator,” in *Proceedings of Austrian Robotics Workshop 2023*, 2023, pp. 1 – 6.

https://doi.org/10.34749/3061-0710.2025.2